[CANCER RESEARCH 64, 5745–5752, August 15, 2004]

Synergistic Tumor Suppression by Coexpression of FHIT and p53 Coincides with FHIT-Mediated MDM2 Inactivation and p53 Stabilization in Human Non-Small Cell Lung Cancer Cells

Masahiko Nishizaki,[1] Ji-ichiro Sasaki,[1] Bingliang Fang,[1] Edward. N. Atkinson,[2] John D. Minna,[3] Jack A. Roth,[1] and Lin Ji[1]

Departments of [1]Thoracic & Cardiovascular Surgery and [2]Biomathematics, University of Texas M. D. Anderson Cancer Center, Houston, Texas, and [3]Department of Internal Medicine and Pharmacology, Hamon Center for Therapeutic Oncology Research, University of Texas Southwestern Medical Center, Dallas, Texas

ABSTRACT

Aberrations of the tumor suppressor genes *FHIT* and *p53* are frequently associated with a wide range of human cancers, including lung cancer. We studied the combined effects of FHIT and p53 proteins on tumor cell proliferation and apoptosis in human non-small cell lung carcinoma (NSCLC) cells *in vitro* and on tumor growth in animal models by adenoviral vector-mediated cotransfer of wild-type *FHIT* and *p53* genes. We found that the coexpression of FHIT and p53 synergistically inhibited tumor cell proliferation in NSCLC cells *in vitro* and suppressed the growth of human tumor xenografts in nude mice. Furthermore, we found that this synergistic inhibition of tumor cell growth corresponded with the FHIT-mediated inactivation of MDM2, which thereby blocked the association of MDM2 with p53, thus stabilizing the p53 protein. Our results therefore reveal a novel molecular mechanism consisting of FHIT-mediated tumor suppression and the interaction of FHIT with other cellular components in the pathways regulating p53 activity. These findings show that combination treatment with synergistic tumor-suppressing gene therapy such as Ad-*FHIT* and Ad-*p53* may be an effective therapeutic strategy for NSCLC and other cancers.

INTRODUCTION

The pathogenesis of lung cancer involves a multistep process of genetic and molecular changes. Genomic aberrations involving human chromosome 3p are the most frequent and earliest genetic events in lung tumorigenesis and may affect several tumor suppressor genes and oncogenes in this region (1). One such tumor suppressor gene is the *FHIT* gene that is located at 3p14.2 and spans the *FRA3B* fragile site, which is very vulnerable to environmental carcinogens and, in human cancer, is frequently involved in allele loss, genomic rearrangement, and cytogenetic abnormalities (2). Indeed, genomic alterations of the *FHIT* gene and resultant deficient expression of the FHIT protein have been associated with many types of human cancers, including those of the lung, breast, cervix, colon, pancreas, stomach, and kidney (2).

The *FHIT* gene encodes a protein composed of 147 amino acids and is a member of the histidine triad (HIT) nucleotide-binding protein superfamily (3). Several lines of experimental evidence, both *in vitro* and *in vivo*, have supported the tumor suppressor role of the *FHIT* gene. For example, the exogenous expression of FHIT protein in FHIT-deficient human cancer cells inhibited tumor cell proliferation *in vitro* (4, 5) and suppressed tumor growth and tumorigenicity *in vivo* (4, 6) by altering the cell cycle and inducing apoptosis. In addition, using an FHIT transgenic mouse model, Fong *et al.* (7) recently noted that the FHIT-heterozygous (+/−) mice developed multiple visceral and skin tumors similar to those seen in patients with Torre's syndrome, which is caused by a deficiency in a mismatch repair gene. Conversely, the reintroduction of the wild-type *FHIT* gene into the FHIT-deficient mice prevented tumor development (8). The molecular mechanism involved in the *FHIT*-mediated tumor-suppressing activities remains to be elucidated, however.

The tumor suppressor gene *p53*, on the other hand, is a well-established cellular gatekeeper that plays an important role in the regulation of numerous biological processes, including cell proliferation, cell cycle progression, apoptosis, and tumor surveillance (9). The *p53* gene is also the most frequently mutated gene in human cancers (10) with >50% of NSCLCs processing a mutation in this gene (11). Transfer of the wild-type *p53* gene, on the other hand, has proved effective in suppressing the proliferation of tumor cells bearing mutated *p53* as seen *in vitro*, in animal models, and in patients with cancer (12–15). However, because many cancer cells, including lung cancer cells, express wild-type *p53* and most tumors are also heterogeneous with respect to their *p53* status, *p53* gene transfer alone may be insufficient to suppress tumor cell growth because of the general resistance of the wild-type *p53*-expressing tumor cells to *p53* gene transfer (12, 14, 16).

Although the efficiency of p53 in preventing cell proliferation is a strong deterrent to malignant progression, the activity of p53 is tightly regulated by divergent extracellular and intracellular signals through the mechanisms that result in degradation, stabilization, or accumulation of p53 protein (9, 17). One protein that plays an essential role in the regulation of p53 is the MDM2 protein, which functions as a ubiquitin ligase for p53 (17–19). Multiple cellular pathways also exist in the regulation of MDM2 activity (17–19). One of the mechanisms that are potentially responsible for the resistance of wild-type p53-expressing tumors to *p53* gene transfer may be imposed via a negative feedback pathway of *p53* and MDM2 in which the introduction of exogenous p53 induces the overexpression of endogenous MDM2, which, in turn, results in rapid degradation of the p53 protein in the ubiquitin-proteasome system (20, 21).

We and others (4, 5) have studied the effects of FHIT and p53 on tumor cell proliferation and apoptosis in the context of diverse biological activities, especially the ability of FHIT to induce apoptosis and alter cell cycle kinetics in various types of cells and the apparent link of the *FHIT* genomic aberrations to the integrity of p53 function in lung tumorigenesis (22). In this study, we used the adenoviral vector-mediated cotransfer of *FHIT* and *p53* in NSCLC cells with a varying p53 status to evaluate the interaction and therapeutic potential of *FHIT* and *p53* gene coexpression by using isobologram modeling. We also sought to elucidate the molecular mechanism involved in the tumor suppression activities mediated by the interaction between

Received 1/20/04; revised 5/4/04; accepted 6/11/04.

Grant support: NIH P01 Grant CA78778-01A1, NIH Specialized Programs of Research Excellence 2P50-CA70970-04, gifts to the Division of Surgery from Tenneco and Exxon for the Core Laboratory Facility, University of Texas M. D. Anderson Cancer Center Support Core Grant CA 16672, a grant from the Tobacco Settlement Funds as appropriated by the Texas State Legislature, and a W. M. Keck Gene Therapy Career Development Grant.

The costs of publication of this article were defrayed in part by the payment of page charges. This article must therefore be hereby marked *advertisement* in accordance with 18 U.S.C. Section 1734 solely to indicate this fact.

Note: M. Nishizaki and J. Sasaki contributed equally to this work

Requests for reprints: Lin Ji, Department of Thoracic and Cardiovascular Surgery, The University of Texas M. D. Anderson Cancer Center, Unit 445, 1515 Holcombe Boulevard, Houston, TX 77030. Phone: (713) 794-1443; Fax: (713) 794-4901; E-mail: lji@mdanderson.org.

FHIT and p53 proteins *in vitro* and *in vivo*. We present here the first evidence that the coexpression of FHIT and p53 synergistically inhibited tumor cell proliferation in both p53-sensitive and p53-resistant NSCLC cell lines *in vitro* and suppressed the growth of p53-resistant tumor xenografts in nude mice. We also demonstrated that the synergism of the FHIT- and p53-mediated tumor-suppressing activity was associated with the FHIT-mediated inactivation of MDM2 and the subsequent stabilization of the p53 protein. Our results provide insight into the interaction of FHIT and p53 and the *FHIT*-mediated inhibition of tumor cell growth and regulation of p53 activity and suggest novel strategies for cancer gene therapy.

MATERIALS AND METHODS

Cell Lines and Cell Culture. Four human NSCLC cell lines, A549, H1299, H322, and H460, with a varied *p53* gene status of and deficiency of FHIT protein expression were used for both *in vitro* and *in vivo* experiments. The A549 line, which contains wild-type p53, was maintained in Ham's F-12 medium supplemented with 10% FCS. The H1299, H322, and H460 lines had an internal homozygous deletion of the *p53* gene, a mutated *p53* gene, and the wild-type *p53* gene, respectively, and were maintained in RPMI 1640 supplemented with 10% FCS and 5% glutamine. Normal human bronchial epithelial cells were obtained from Clonetics, Inc. (Walkersville, MD), and cultured in the medium supplied by the manufacturer according to the instructions provided. The normal human lung fibroblast line WI-38 and immortalized human bronchial epithelial cells were maintained in MEM Earle's BSS with 10% fetal bovine serum and 5% glutamine and used as normal cell control. All cells were incubated in a humidified incubator supplied with 5% carbon dioxide. All cell cultures were tested regularly for possible microplasma contamination.

Adenoviral and Plasmid Vectors. Recombinant adenoviral vectors Ad-*p53* and Ad-*FHIT*, which contain the wild-type *p53* gene and an *FHIT* gene, respectively, were used as gene therapy agents, and either Ad-*LacZ*, which contains a *β-galactosidase* gene, or Ad-*GFP* was used as a nonspecific negative control. Construction of these recombinant adenoviral vectors has been described previously (4). Viral stocks were prepared by the Vector Core Facility at The University of Texas M. D. Anderson Cancer Center (Houston, TX). Viral titers were determined by absorbance measurements (viral particles/ml) and plaque assays (plaque forming units/ml). Potential contamination of the viral preparations by a wild-type virus was monitored by PCR analysis. Expression plasmid vectors containing the cDNA of *FHIT*, *HDM2*, *LacZ*, and *GFP* genes were used to transfect NSCLC cells using a FuGENE 6 transfect reagent (Roche Molecular Biochemicals, Indianapolis, IN).

Immunofluorescence Staining. Cells were first cultured in chamber slides and treated with adenoviral vectors at various multiplicities of infection (MOI) for 24 h. Cells were then fixed with 4% paraformaldehyde in PBS (pH 7.4) for 30 min on ice. Cells were rinsed twice with PBS and permeabilized with 0.2% Triton X-100 for 10 min. For immunostaining, cells were incubated with rabbit anti-FHIT (Zymed Laboratories, South San Francisco, CA) and mouse anti-p53 or anti-MDM2 (Santa Cruz Biotechnology, Santa Cruz, CA) antibodies diluted in PBS containing 5% BSA for 1 h at room temperature. FITC-labeled antirabbit IgGs and rhodamine-labeled antimouse IgGs (Chemicon International, Temecula, CA) were diluted 1:200 in PBS, and the cells were incubated with the antibodies for 30 min. The nuclei were stained by 4′,6-diamidino-2-phenylindole and then examined under an Eclipse E400 fluorescence microscope (Nikon, Tokyo, Japan) equipped with a Sensys digital camera (Photometrics, Tucson, AZ) and Metamophore software (Universal Imaging Corp., Downingtown, PA).

Growth Inhibition and 2,3-Bis[2-methoxy-4-nitro-5-sulfophenyl]-2*H*-Tetrazolium-5-Carboxanilide Inner Salt Assay. Inhibition of tumor cell growth by adenoviral vector-mediated transfer of *FHIT* and *p53* genes was analyzed by quantitatively determining cell viability using an improved 2,3-bis[2-methoxy-4-nitro-5-sulfophenyl]-2*H*-tetrazolium-5-carboxanilide inner salt assay (Roche Molecular Biochemicals). PBS was used as a mock control and Ad-*LacZ* as a negative control. Briefly, cells were plated in 96-well microtiter plates at 1×10^3 cells/well in 100 μl of medium. One day after the cells were plated, 25-μl aliquots of medium containing adenoviral vectors at various MOI (viral particles/cell) were added. Cells were then incubated at 37°C in a humidified atmosphere under 5% CO_2. Four days after transduction, cell viability was quantified in a microplate reader (Model MRX; Dynatech Laboratories, Chantilly, VA) by a 2,3-bis[2-methoxy-4-nitro-5-sulfophenyl]-2*H*-tetrazolium-5-carboxanilide inner salt assay according to the manufacturer's instructions. The percentage of viable cells was calculated in terms of the absorbency in treated cells relative to the absorbency in untreated control cells. Experiments were repeated at least three times and triplicate samples were used for each treatment.

Isobologram Analysis of the Interaction of FHIT and p53. The effects of the coexpression of two tumor suppressor genes, *FHIT* and *p53*, on tumor cell growth in five human cell lines (WI-38, H1299, H460, H322, and A549) were analyzed quantitatively and statistically *in vitro* by the improved isobologram method of Steel and Peckham (23). The mathematical operation and statistical analysis methods have been described elsewhere (23, 24). The MOI for the cotransduction were based on the IC_{50} values determined from each individual vector in different cell lines (Table 1). An equal amount of viral particles from each of the two vectors in cotransduction experiment is used to bring the total viral particles to the same amount as those in a single vector transduction.

Apoptosis and Cell Cycle Kinetics Assay. Cells were transduced with adenoviral vectors at various MOI based on the ID_{50} values (Table 1). Seventy-two h after transduction, cells were collected, fixed in 4% paraformaldehyde, permeabilized with 70% ethanol, washed with PBS, and stained with propidium iodide solution containing 40 μg/ml propidium iodide and 10 μg/ml DNase-free RNase A. DNA fragmentation was analyzed by flow cytometry. The percentage of apoptotic cells was shown by the cells in the G_0-G_1 phase.

Immunoprecipitation, Immunodepletion, and Western Blot Analysis. For the preparation of crude cell lysates, cells were suspended in immunoprecipitation SDS-PAGE running buffer (radioimmunoprecipitation assay) containing 1% NP40, 0.5% sodium deoxycholate, 0.1% SDS, and a complete set of proteinase inhibitors (Roche Molecular Biochemicals) and lysed for 20 min at 4°C. Cell lysates were passed through a 25-gauge needle and briefly sonicated twice for 30 s each. Protein concentrations were determined using the Bio-Rad protein assay (Bio-Rad Laboratories, Hercules, CA). For the immunoprecipitation studies, cell lysates were precleared by incubation with 10 μl of protein A/G-agarose (Santa Cruz Biotechnology, Inc.) for 30 min at 4°C and then centrifugation. Each protein sample (500 μg) was incubated with its respective antibody at 4°C overnight, followed by incubation with 25 μl of A/G-agarose beads. After centrifugation, the resultant supernatant was saved as an immunodepleted fraction. The precipitated beads were then washed three times in radioimmunoprecipitation assay buffer and once in PBS. The bound proteins were solubilized by adding 25 μl of SDS-containing sample buffer. The crude cell lysates and the immunoprecipitated and immunodepleted samples were used in standard SDS-PAGE and Western blot analyses.

Quantitative Real-time Reverse Transcription-PCR (RT-PCR). The TaqMan probe and primers for the *MDM2* gene were designed using Primer-express software (Perkin-Elmer Applied Biosystems, Foster City, CA) and synthesized by the same manufacturer. The human genomic DNA or total RNAs were used as template standards, and the human β-actin or glyceraldehyde-3-phosphate dehydrogenase TaqMan probes and primers were used as their respective internal controls. Total RNAs were isolated from Ad-*FHIT*- and Ad-*p53*-transduced tumor cells using Trizol reagent (Life Technologies, Inc., Grand Island, NY), as instructed by the manufacturer, and RNA samples were treated with DNase (Life Technologies, Inc.). Real-time RT-PCR and the quantification of RT-PCR products were performed and the products analyzed using a TaqMan Gold RT-PCR Kit, an ABI Prism 7700 Sequence Detection System, and the appropriate software according to the manufacturer's instructions (Perkin-Elmer Applied Biosystems).

Efficacy of Combination Treatment with Ad-*FHIT* and Ad-*p53* in Animal Models. All animals were maintained and animal experiments performed according to NIH and institutional guidelines established for the Animal Core Facility at M. D. Anderson. The animals used in this study were female *Nu/nu* mice (6–8 weeks of age) that were purchased from Charles River Laboratories (Wilmington, MA). Before tumor cell inoculation, mice were subjected to 3.5 Gy of total body irradiation from a ^{137}Cs radiation source.

A549 cells were used to establish s.c. tumors in mice. Briefly, 1×10^6 cells were injected into the right flank of each mouse. When the average size of the xenograft tumors reached 5–8 mm in diameter, the mice were randomly divided into six treatment groups: PBS control; single treatments with Ad-

Table 1 *p53 status of NSCLC cell lines, ID_{50} values and combination effects of Ad-p53, Ad-FHIT, and Ad-LacZ*

Cell line	Histologic subtype	p53 status	ID_{50} value (MOI)			Combination effects		
			Ad-*p53*	Ad-*FHIT*	Ad-*LacZ*	Ad-*p53* + Ad-*FHIT*	Ad-*p53* + Ad-*LacZ*	Ad-*FHIT* + Ad-*LacZ*
H1299	LC	Null	120.7 ± 21.70	702.8 ± 49.16	3,669.0 ± 37.96	Synergy ($P = 0.0117$)	Additive	Additive
H322	AD	Mutant	2,608.6 ± 16.40	1,582.9 ± 30.04	8,907.7 ± 189.06	Synergy ($P = 0.0181$)	Additive	Additive
H460	LC	Wild-type	6,815.3 ± 72.31	4,932.4 ± 91.46	14,298.3 ± 446.02	Synergy ($P = 0.0051$)	Additive	Additive
A549	AD	Wild-type	3,052.8 ± 96.60	1,778.7 ± 149.57	9,273.4 ± 224.93	Synergy ($P = 0.0117$)	Additive	Additive
Wi-38	NLF	Wild-type	7,920.24 ± 54.21	56,530.5 ± 250.38	UD	Additive	UD	UD

Abbreviations: MOI, multiplicity of infection, expressed as viral particles/cell; LC, large cell carcinoma; AD, adenocarcinoma; NLF, normal lung I fibroblast; UD, undetermined.

FHIT, Ad-*p53*, or Ad-*LacZ* vector alone; and combination treatment with Ad-*p53* + Ad-*FHIT* and Ad-*p53* + Ad-*LacZ*. Each treatment group contained eight mice, and experiments were repeated twice.

Mice were treated according to the following schedule: on day 0, each mouse was injected intratumorally with adenoviral vector (Ad-*p53*, Ad-*FHIT*, or Ad-*LacZ*) at a dose of 3×10^{10} viral particles/tumor in a volume of 0.2 ml. Ear tags were placed on the mice so that data obtained from individual animals could be traced. Tumor dimensions were measured three times/week using a digital caliper.

Statistical and Mathematical Analyses. Tumor volume was calculated using the equation $V\ (mm^3) = a \times b^2/2$, where a is the largest diameter, and b is the smallest diameter. Differences in tumor volumes between treatment groups were analyzed using the ANOVA test and statistical software. A difference was considered to be statistically significant when $P \leq 0.05$.

A mathematical model and a statistical method were developed to analyze the effects of combination treatments in our animal model according to the improved isobologram method of Steel and Peckham (23–25) Tumor volumes (V) were fitted with dose-response curves f_a(Da) for reagent A and f_b(Db) for reagent B by the following equations: $V = f_a(\mathrm{Da})$ and $V = f_b(\mathrm{Db})$. Then mode I, mode IIa, and mode IIb could be expressed as follows: $V_{\mathrm{Mode\ I}} = f_a(D_a) \times f_b(D_b)$; $V_{\mathrm{Mode\ IIa}} = fb[_{fb}{}^{-1}f_a(D_a) + D_b]$; and $V_{\mathrm{Mode\ IIb}} = fa[f_a{}^{-1}f_b(D_b) + D_a]$. The range of additivity was defined as being between the maximum (V_{max}) and minimum (V_{min}) tumor volume among these three isoeffect volumes: $V_{\mathrm{Mode\ I}}$, $V_{\mathrm{Mode\ IIa}}$, and $V_{\mathrm{Mode\ IIb.}}$ When the observed tumor volume after combination treatment was between V_{max} (boundary between addition and antagonism) and V_{min} (boundary between addition and synergism), the treatment combination effect was regarded as additive. When the observed tumor volume after combination treatment was below V_{min} or above V_{max}, the effect was regarded as synergistic or antagonistic, respectively. The Wilcoxon signed rank test was used for statistical analysis, and $P < 0.05$ was taken to indicate a significant difference.

RESULTS

Coexpression of FHIT and p53 Inhibits NSCLC Cell Proliferation. The wild-type *FHIT* and *p53* genes were coexpressed in human NSCLC cells by recombinant adenoviral vector-mediated gene transfer to study the combined effects of FHIT and p53 proteins on tumor cell proliferation. The coexpression of the FHIT and p53 proteins was detected by immunofluorescence staining in H1299 and A549 cells cotransduced with Ad-*FHIT* and Ad-*p53* (Fig. 1*A*). In particular, the fluorescence images showed nuclear staining (4′,6-diamidino-2-phenylindole, blue) and cytoplasmic and nuclear staining for FHIT (FITC, green) and p53 (rhodamine, red) in H1299 cells (Fig. 1*A*, *a–d*) and A549 cells (Fig. 1*A*, *e–h*) 24 h after the cotransduction of Ad-*p53* and Ad-*FHIT*. Specifically, the coexpression of FHIT and p53 was seen in 97.6% of H1299 cells and 95.4% of A549 cells. χ^2 statistical analysis showed that these coincidences of the expression of both proteins in both types of cells were significant ($P < 0.001$), indicating that equivalent levels of expression of both the FHIT and p53 proteins could be achieved in transduced cells.

Next, the effect of FHIT and p53 expression on tumor cell proliferation was determined in four NSCLC cell lines by analyzing the relative viability of cells transduced by the Ad-*FHIT* and Ad-*p53* vectors alone or in combination: H1299 (*p53* null); H322 (mutant *p53*); H460 (wild-type *p53*); and A549 (wild-type *p53*) cells. The Ad-*LacZ* vector was used as a nonspecific control for gene transfer. Endogenous expression of the FHIT protein could not be detected in any of the cell lines.

The dose effect of each agent on tumor cell proliferation was then subjected to the median-effect equation to generate dose-response curves (24). The ID_{50} values (doses of adenoviral vectors that inhibited cell growth by 50%) were then determined on the basis of the resultant dose-response curves (Table 1). The responses of NSCLC cell lines to Ad-*p53* or Ad-*FHIT* varied from the most sensitive (low ID_{50}) to the most resistant (high ID_{50}) in the following orders of sensitivity: H1299 > H322 > A549 > H460 (Table 1). Although Ad-*LacZ* had a detectable inhibitory effect on cell proliferation, the effect was significantly less than that of Ad-*FHIT* or Ad-*p53*, and ID_{50} values of Ad-*LacZ* could be determined only at a very high dose (Table 1), supporting the specificity of FHIT- and p53-mediated tumor suppression activities.

The combined effects of FHIT and p53 on cell proliferation were evaluated by isobolograms generated (Fig. 1*B*) using averaged data from experiments done independently at least twice for all cell lines tested. Combination treatment with Ad-*FHIT* + Ad-*p53* exhibited a synergistic antiproliferative effect in all cancer cell lines tested independent of their *p53* status, whereas no synergistic effect was observed in normal human lung fibroblasts WI-38 cells (Fig. 1*B*). On the other hand, the combination of either Ad-*p53* + Ad-*LacZ* (Fig. 1*B*, *middle panels*) or Ad-*FHIT* + Ad-*LacZ* (Fig. 1*B*, *bottom panels*) showed no synergistic effects in any of the cancer cell lines. A nonparametric statistical analysis of the predicted data *versus* the observed data showed that the observed synergistic effects on tumor cell proliferation of Ad-*FHIT* + Ad-*p53* were statistically significant in all cancer cell lines (H1299, $P = 0.0117$; H322, $P = 0.0181$; H460, $P = 0.0051$; A549, $P = 0.0117$; Table 1).

Effects of Coexpression of FHIT and p53 on Apoptosis. One of the hallmark molecular events induced by tumor suppressors is apoptosis. To study the combined effects of FHIT and p53 on apoptosis, suboptimal doses (slightly lower than the ID_{50} values in each NSCLC line shown in Table 1) of Ad-*FHIT* and Ad-*p53* vectors were applied to each cancer cell line. For the combination treatment, the ratio of the MOI (viral particles/cell) of Ad-*FHIT* to Ad-*p53* was 500:50 in the H1299 cells and 2500:2500 in the H460, normal human bronchial epithelial, and WI-38 cells. For the single treatment, either Ad-*FHIT* or Ad-*p53*, an appropriate amount of Ad-*LacZ* vectors, was added to make the total viral particles equal to that of the combination treatment.

The apoptosis and cell-cycle kinetics in cells transduced with Ad-*FHIT* and Ad-*p53* were then analyzed by flow cytometry in conjunction with propidium iodide staining (Fig. 1*C*). The accumulation of cells in the sub-G_0-G_1 phase analyzed with propidium iodide staining was correlated with positive cells analyzed with terminal deoxynucleotidyl transferase-mediated nick end labeling staining by flow cytometry. A low level of apoptosis was observed in the H1299 and H460 cells transduced with Ad-*FHIT* alone at 72 h after posttranduction (Fig. 1*C*). An intermediate level was seen in the cells transduced with Ad-*p53* alone (Fig. 1*C*). However, a supra-additive

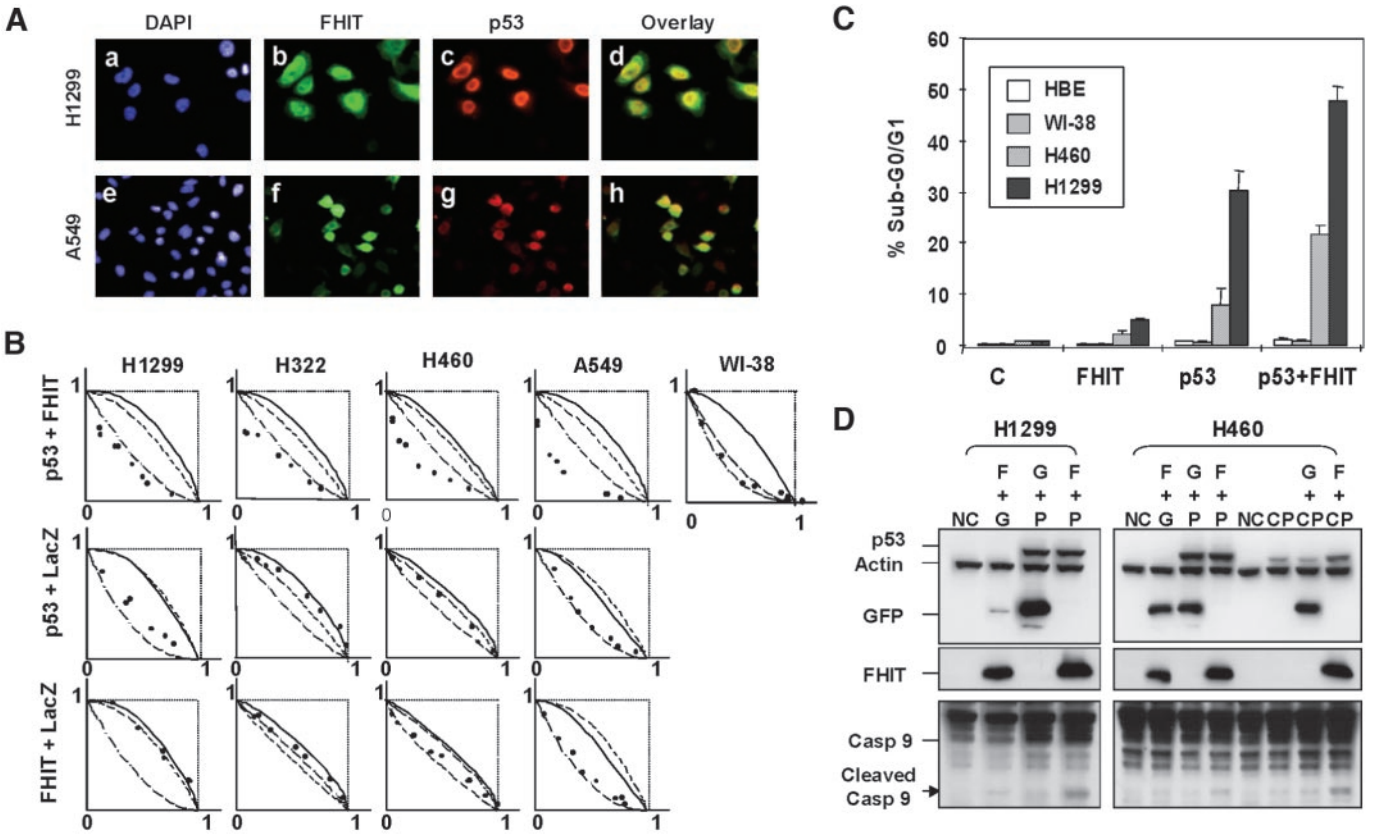

Fig. 1. Effects of coexpression of FHIT and p53 on the growth and apoptosis of NSCLC cells. *A*, immunofluorescence analysis of the expression of FHIT and p53 proteins in NSCLC cells cotransduced with Ad-*FHIT* and Ad-*p53* vectors. Immunofluorescence staining was performed on H1299 (*a–d*) and A549 (*e–h*) cells 24 h after transduction. Nuclei were stained by 4′,6-diamidino-2-phenylindole (DAPI; *blue*, *a* and *e*). Expression of FHIT proteins is shown in *green* (*b* and *f*), and expression of p53 proteins is shown in *red* (*c* and *g*). Immunofluorescence images were overlapped to confirm the coexpression of FHIT and p53 (*yellow*, *d* and *h*). *B*, evaluation of effects of coexpression of FHIT and p53 on the growth of NSCLC cells and normal lung fibroblasts (WI-38) shown by isobologram analysis at the ID_{50} level. The envelope of additivity in each isobologram is defined by three predicted isoeffect lines, and the observed data are plotted by ●. If the observed data are distributed inside, above, or below the envelope of additivity, the interaction is considered additive, antagonistic, or synergistic, respectively. The interaction of the gene therapy combination (Ad-p53 + Ad-FHIT, Ad-p53 + Ad-LacZ, and Ad-FHIT + Ad-LacZ) in each cell line is demonstrated by individual isobolograms. Statistical analysis was performed using the Wilcoxon signed rank test. $P \leq 0.05$ was considered significant (see "Materials and Methods"). *C*, the effect of overexpression of FHIT and p53 on apoptosis and cell cycle kinetics in Ad-*FHIT*- and Ad-*p53*-transduced NSCLC cells. DNA fragmentation and cell cycle kinetics in various NSCLC cells transduced with Ad-*FHIT* and Ad-*p53* alone or in combination were analyzed by flow cytometry in conjunction with propidium iodide staining. PBS was used as a control. The percentages of apoptotic cells are represented by G_0-G_1 cells in the sub-G_0-G_1 phase. *D*, Western blot analysis to assess FHIT-mediated p53 protein stabilization and caspase-9 activation. H1299 cells were cotransfected with Ad-*FHIT* and Ad-*p53* vectors for 72 h, and H460 cells were pretreated with 2 μM cisplatin for 24 h and then transduced with Ad-*FHIT* for 48 h. The cleaved caspase-9 products are indicated by an *arrow*. NC, negative control with PBS; F, Ad-*FHIT*; G, Ad-*GFP*; P, Ad-*p53*; and CP, cisplatin.

induction of apoptosis was seen in these same cell lines when they were cotransduced with Ad-*FHIT* and Ad-*p53*, but no significant enhancement of apoptosis was observed in normal cell lines cotransduced with Ad-*FHIT* and Ad-*p53* at the same viral doses and at the same time after transduction (Fig. 1*C*).

Consistent with the flow cytometry results, caspase-9 was also found to be activated in the H1299 and H460 cells transduced with either Ad-*FHIT* or Ad-*p53* alone or in combination, as shown by the cleavage products detected by Western blot analysis (Fig. 1*D*). In addition, caspase-9 was strongly activated in H460 cells (wild-type p53) in which the endogenous p53 was activated by cisplatin treatment followed by the transduction with Ad-*FHIT* (Fig. 1*D*, *Lane F+CP*) as compared with the effects in cells transduced with Ad-*GFP* (Fig. 1*D*, *Lane G+CP*). These results suggest that the observed synergism in the inhibition of tumor cell proliferation produced by the coexpression of FHIT and p53 is due to a synergistic induction of apoptosis.

Synergistic Inhibition of Tumor Growth by the Coadministration of Ad-*p53* and Ad-*FHIT in Vivo*. To determine whether the synergistic growth inhibition mediated by the cotransfer of the *FHIT* and *p53* genes observed *in vitro* could be reproduced *in vivo*, we evaluated the combined effects of FHIT and p53 overexpression on tumor growth by directly coadministering Ad-*FHIT* and Ad-*p53* vectors into human A549 s.c. xenografts in nude mice. Mice were divided into six treatment groups: four groups that received single treatment with PBS; Ad-*LacZ*, Ad-*p53*, or Ad-*FHIT* alone; and combinations of Ad-*p53* + Ad-*FHIT* or Ad-*p53* + Ad-*LacZ*. Each treatment group contained five to eight mice, and all experiments were repeated twice. The overall effects of treatments on tumor growth were analyzed by an ANOVA statistical method. Treatment with Ad-*p53* + Ad-*FHIT* significantly inhibited tumor growth in the A549 tumor model ($P < 0.05$) in comparison with the results seen in the other treatment and the control groups (Fig. 2*A*). We also analyzed whether there was a synergistic interaction between the combination treatment elements in these tumors using a modified isobologram method (see "Materials and Methods"). This showed that coadministration of Ad-*p53* and Ad-*FHIT* produced a significant synergistic inhibitory effect on tumor growth in the A549 tumor model ($P < 0.05$; Fig. 2*B*).

Stabilization of p53 Protein by FHIT Overexpression. To elucidate the molecular mechanisms responsible for the synergistic inhibitory effects of coexpression of FHIT and p53 on tumor growth, we studied their mutual effects on the accumulation and stability of the FHIT and p53 proteins themselves in Ad-*FHIT*- and Ad-*p53*-transduced NSCLC cells using Western blot analysis (Fig. 3, *A* and *B*). The overexpression of FHIT up-regulated the expression of endogenous wild-type p53 proteins >6-fold in Ad-*FHIT*-transduced H460 and

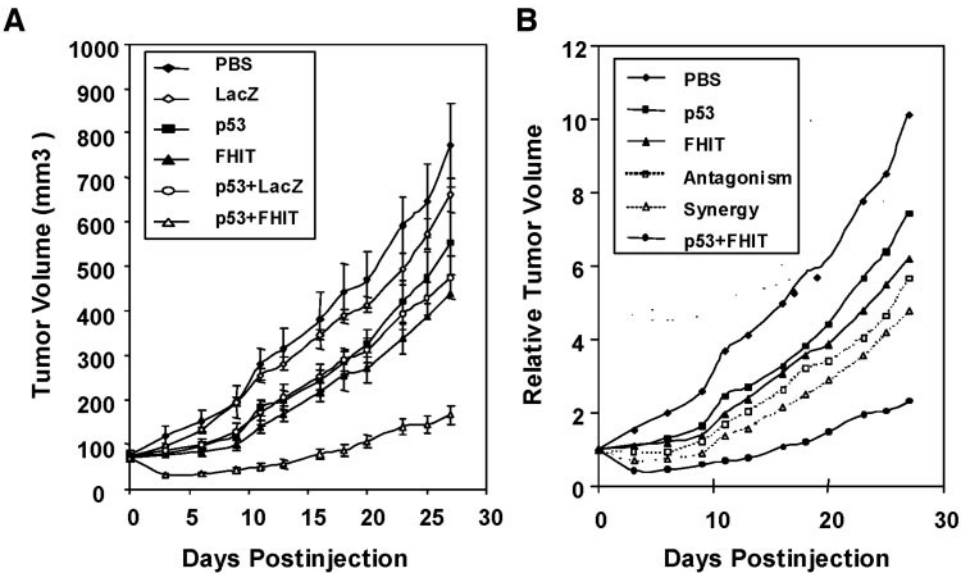

Fig. 2. Suppression of tumor growth by the coadministration of Ad-*p53* and Ad-*FHIT* vectors in human A549 xenografts in nude mice. *A*, effects on tumor growth. Results are reported as the mean ± SE. The tumors in the mice treated with the combination of Ad-*p53* + Ad-*FHIT* vectors were significantly smaller than those in the other groups ($P < 0.05$). *B*, analysis of synergism in tumors in which both Ad-*FHIT* and Ad-*p53* were administered. The combined effects of FHIT and p53 expression on tumor growth were analyzed using a modified isobologram method (see "Materials and Methods"). The predicted boundaries between the additive and antagonistic effects and between the additive and synergistic effects of combination treatments on tumor volumes are indicated by the *dashed line* with □ and the *dashed line* with △, respectively. Results are reported as the mean of relative tumor volumes. The inhibition of tumor growth by combination treatment with Ad-*p53* + Ad-*FHIT* is significantly synergistic ($P = 0.0033$).

A549 cells but not in the H322 cells with endogenous mutant p53 (Fig. 3*A*). A modest increase of exogenous p53 was also seen in Ad-*p53* and Ad-*FHIT* cotransduced cells, independent of the endogenous *p53* status in these cells (Fig. 3*B*). However, the level of the exogenous FHIT protein was not affected by either the endogenous or exogenous expression of p53 (Fig. 3*A*, *middle panels*), suggesting that the synergistic effect of the tumor suppressor genes may be due to FHIT-mediated up-regulation of the p53 protein but not the reverse.

To confirm that the increased level of p53 protein induced by FHIT is due to protein stabilization, we performed a protein synthesis inhibitor cyclohexamide-mediated pulse-chase Western blot analysis to monitor the endogenous p53 expression and protein turnover induced by pretreatment with cisplatin in the presence or absence of Ad-*FHIT*. In the absence of Ad-*FHIT*, the level of the p53 protein was dramatically reduced at 6 h and almost not detectable at 15 h after cyclohexamide treatment (Fig. 3*C*, PBS). By comparison, in the presence of exogenous Ad-*FHIT*, the endogenous p53 protein in these cells could still be detected even 24 h after cyclohexamide treatment (Fig. 3C, Ad-*FHIT*). These results indicate that expression of FHIT protein indeed stabilizes the p53 protein.

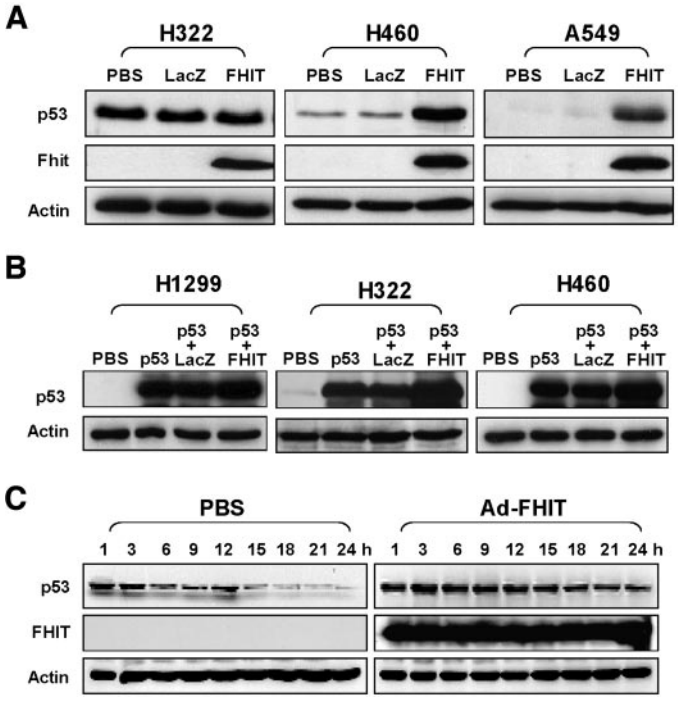

Fig. 3. Western blot analysis of p53 expression in Ad-*FHIT*-transduced NSCLC cells. The endogenous (*A*) and exogenous (*B*) expression of p53 proteins was probed by immunoblotting with a mouse monoclonal anti-p53 antibody. FHIT expression (*A*) was probed with rabbit anti-FHIT antibodies. *C*, effect of FHIT on endogenous p53 protein stability shown by cyclohexamide-mediated pulse-chase Western blot analysis. A549 cells were pretreated with 2 μM cisplatin at 24 h before 10 μM cyclohexamide with or without Ad-*FHIT* transduction. Cell extracts were then harvested at the indicated times.

Regulation of the *MDM2* by Coexpression of FHIT and p53. There are multiple pathways to stabilize p53 in response to different forms of stress. One of the key pathways is to inhibit MDM2-mediated p53 degradation by dissociating MDM2 from p53 (21, 26). To determine whether the enhanced stability of p53 is associated with the inactivated MDM2 in NSCLC cells cotransduced with Ad-*FHIT* and Ad-*p53*, we analyzed the expression of MDM2 proteins by Western blot analysis using a monoclonal MDM2 antibody (SMP-14; Santa Cruz Biotechnology, Inc.; Fig. 4*A*). We detected significantly decreased level of the 90-kDa MDM2 protein in the cells cotransduced with Ad-*FHIT* and Ad-*p53* in comparison with control cells treated with Ad-*p53* alone or with Ad-*p53* + Ad-*LacZ* (Fig. 4*A*) in all cell lines tested. Similar results were observed when MDM2 antibodies from different sources were used (N-20 from Santa Cruz Biotechnology, Inc., and IF2 from Oncogene, Cambridge, MA; data not shown).

To determine whether the reduction in the MDM2 protein was resulted from a transcriptional or posttranscriptional event, we analyzed *MDM2* mRNA transcription using a quantitative real-time RT-PCR in Ad-*FHIT*- and Ad-*p53*-transduced cells (Fig. 4*B*). Transcription of the *MDM2* mRNA was significantly up-regulated in both the Ad-*p53*-transduced and Ad-*FHIT* + Ad-*p53*-cotransduced cells but not in the cells transduced with Ad-*FHIT* alone (Fig. 4*B*). These results suggest that the overexpression of p53 activates *MDM2* at the transcriptional level through a feedback mechanism but that the FHIT-mediated regulation of MDM2 expression occurs at the posttranscriptional protein level.

To exclude the possibility that the adenoviral vector and p53 expression might have affected MDM2 expression, we analyzed the effect of FHIT expression on exogenous MDM2 expression in *p53*-null H1299 cells cotransfected with the *HDM2* and *FHIT* expressing

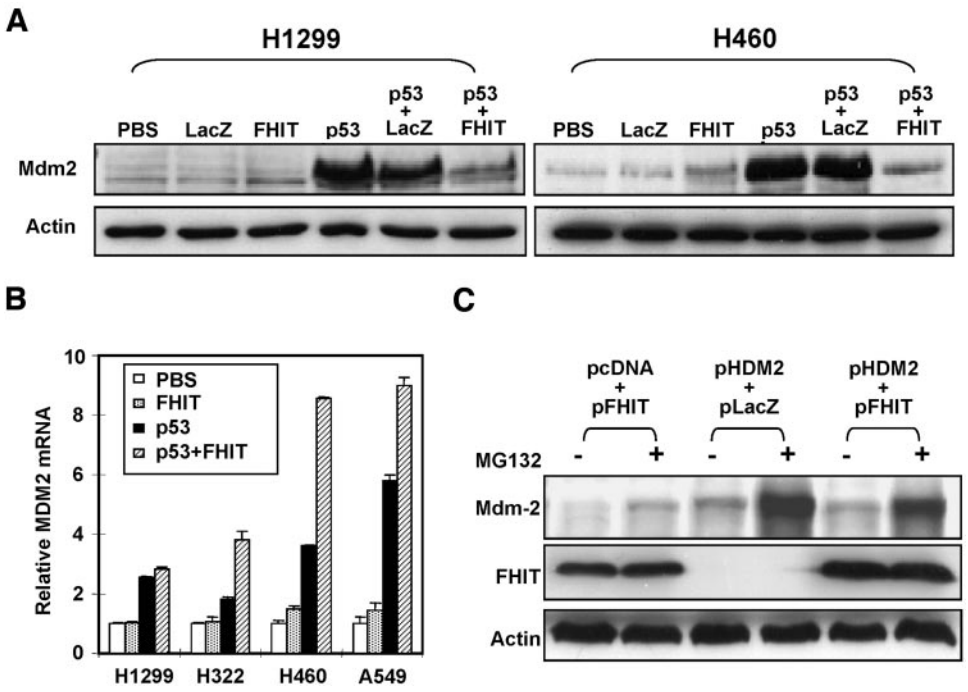

Fig. 4. Modulation of MDM2 expression in NSCLC cells transduced by *Ad-FHIT* and Ad-*p53*. *A*, Western blot analysis of the expression of MDM2 protein. Cells were transduced with *Ad-LacZ*, *Ad-FHIT*, or *Ad-p53* or cotransduced with Ad-*LacZ* + Ad-*p53* or Ad-*FHIT* + Ad-*p53* for 72 h. Cell extracts were analyzed by immunoblotting with a mouse anti-MDM2 monoclonal antibody. *B*, real-time RT-PCR analysis of MDM2 mRNA transcription. Total RNAs were isolated from cells transduced with Ad-*FHIT* or Ad-*p53* or cotransduced with Ad-*p53* + Ad-*FHIT* for 72 h. Real-time RT-PCR was performed with an MDM2 mRNA-specific TaqMan probe and primers on an ABI Prism 7700 Sequence Detection System, and PCR products were analyzed with the software the system was equipped with. *C*, effect of FHIT expression on exogenous MDM2 protein expression in H1299 cells cotransfected with the plasmid vectors pHDM2 and pFHIT. An empty backbone plasmid pcDNA was used as a control. Cells were preincubated with either DMSO or 5 μM MG132 for 3 h and then transfected with various combinations of plasmid vectors. Cells were harvested 48 h after transfection for the preparation of protein lysates.

plasmid vectors (*pHDM2* and *pFHIT*). H1299 cells cotransfected with *pHDM2* and *pLacZ* were used as the control. Consistent with the results obtained in the adenoviral vector-mediated *FHIT* gene transfer experiment (Fig. 4*A*), the level of exogenous MDM2 protein was also reduced in the cells cotransfected with *pHDM2* and *pFHIT* plasmids, compared with the levels in cells cotransfected with *pHDM2* and *pLacZ* (Fig. 4*C*). Furthermore, MDM2 proteins were clearly detected at a similar rate of recovery after treatment with a broad proteasome inhibitor, MG132, in all treatment groups (Fig. 4*C*), suggesting that the FHIT-mediated reduction in the MDM2 protein is independent of the proteasome degradation pathway.

Interruption of Association of MDM2 with p53 by FHIT. To further our understanding of the mechanism behind the observed stabilization of the p53 protein by FHIT, we investigated the interactions among the FHIT, MDM2 and p53 proteins in Ad-*FHIT*- and Ad-*p53*-transduced wild-type *p53*-bearing H460 and A549 cells using immunoprecipitation and Western blot analysis (Fig. 5). The FHIT protein was detected in MDM2-immunoprecipitated complexes in both H460 (Fig. 5*A*, *Lane 2*) and A549 (Fig. 5*A*, *Lane 6*) cells transduced with *FHIT*, indicating a direct interaction between the FHIT and MDM2 proteins. In addition, a significantly smaller amount of the FHIT/MDM2 complexes was observed in both H460 (Fig. 5*A*, *Lane 4*) and A549 (Fig. 5*A*, *Lane 8*) cells that were cotransduced with *Ad-FHIT* + *Ad-p53*. These results suggest that FHIT may cause degradation of MDM2 as implied by the reduced MDM2 levels in Ad-*FHIT* + Ad-*p53*-transduced cells (Fig. 4*A*) and that a large amount of p53 proteins may also interfere with the apparent FHIT-MDM2 interaction.

To determine whether the association of FHIT with MDM2 could interfere with the interaction of MDM2 with p53, we performed a MDM2 immunoprecipitation and MDM2 immunodepletion analysis followed by immunoblotting against p53 protein on denatured cell lysates from Ad-*FHIT*- and Ad-*p53*-transduced cells (Fig. 5*B*). We found that MDM2-bound p53 was detected in the MDM2-immunoprecipitated complexes in both H460 (Fig. 5*B*, *Lane 1*) and A549 (Fig. 5*B*, *Lane 3*) cells transduced with Ap-*p53*. However, the levels of MDM2-bound p53 protein were dramatically reduced in both H460 (Fig. 5*B*, *Lane 2*) and A549 (Fig. 5*B*, *Lane 4*) cells cotransduced with Ad-*FHIT* + Ad-*p53* vectors compared with the levels in cells transduced with Ad-*p53* alone. Furthermore, Western blot analysis of p53 proteins in MDM2-immunodepleted crude protein fractions showed that almost all of the p53 protein was associated with MDM2 in the absence of FHIT expression (Fig. 5*B*, *Lanes 5* and *7*), but the MDM2-p53 protein interaction was significantly interrupted by the presence of FHIT coexpression (Fig. 5*B*, *Lanes 6* and *8*). These results strongly suggest that the interaction of FHIT with MDM2 effectively blocks the association of MDM2 with p53, and this prevented the MDM2-mediated degradation thus enhancing the stability of p53 protein.

We also performed immunofluorescence image analysis of FHIT and MDM2 protein expression to study the interaction of these two proteins in living A549 cells in which endogenous p53 expression was induced by cisplatin and exogenous FHIT expression was induced by Ad-*FHIT* (Fig. 5*C*). In the Ad-*FHIT*-transduced cells (Fig. 5*C*, *a* and *b*), the FHIT protein was detected mainly in the cytosol (Fig. 5*C*, *a*), and the MDM2 protein was predominantly located in the nucleus (Fig. 5*C*, *b*). In untransduced cells (Fig. 5*C*, *b*), MDM2 protein expression could also be detected in the cytosol, but this was not seen in the FHIT-expressing cells (Fig. 5*C*, *b*). In addition, the fluorescence intensity of the MDM2 protein was reduced in nuclei in the FHIT-expressing cells compared with the intensity in the non-FHIT-expressing cells, indicating that a FHIT-mediated reduction in MDM2 protein expression and a FHIT-mediated interference in the association of MDM2 with p53 occurred in living cells.

DISCUSSION

In this study, we investigated the interaction of FHIT and p53 by recombinant adenoviral vector-mediated *FHIT* and *p53* tumor suppressor gene cotransfer in human NSCLCs *in vitro* and *in vivo*. We used improved isobologram modeling and statistical analysis to quantitatively evaluate the mutual effects of *FHIT* and *p53* coexpression on tumor cell proliferation *in vitro* and tumor growth in animal models and demonstrated that the coexpression of FHIT and p53 resulted in

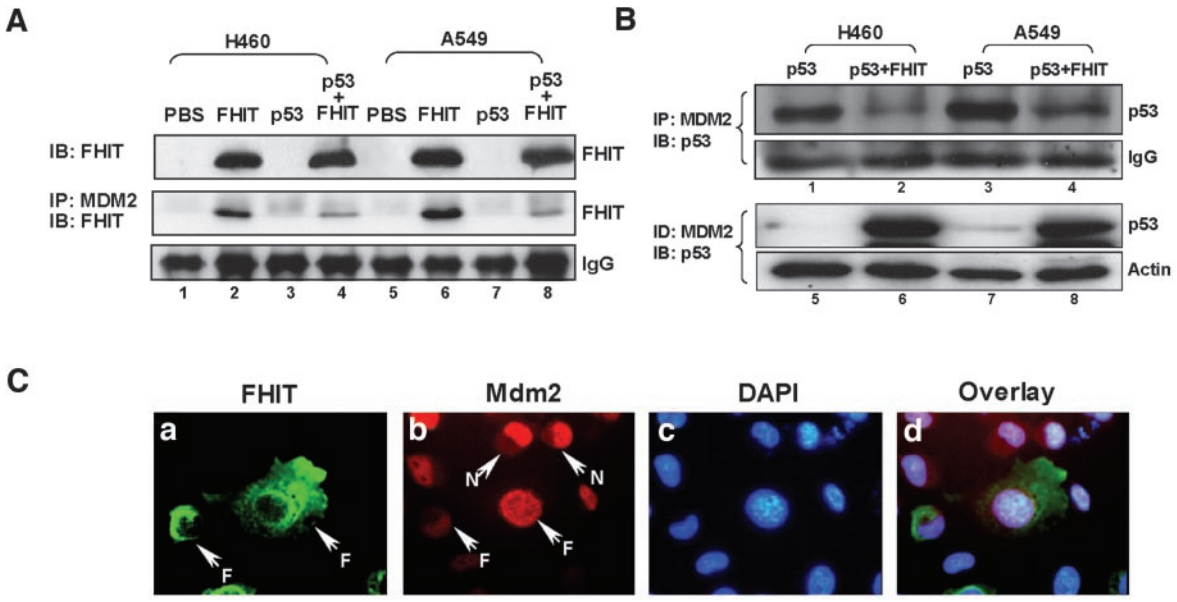

Fig. 5. Immunoprecipitation and immunoblot analysis for the interaction of FHIT, MDM2, and p53 proteins in NSCLC cells. *A*, interaction of FHIT with MDM2 proteins in the presence and absence of exogenous p53 protein expression in H460 and A549 cells. Cell extracts were prepared from cells transduced with Ad-*FHIT* or Ad-*p53* alone or in combination for 72 h. Cell extracts were immunoblotted (IB) with FHIT antibodies and then immunoprecipitated (IP) with a monoclonal MDM2 antibody followed by immunoblotting with polyclonal FHIT antibodies. *B*, effect of FHIT expression on the interaction of MDM2 with p53 proteins in H460 and A549 cells. Tumor cells were transduced with Ad-*p53* alone or cotransduced with Ad-*FHIT* + Ad-*p53* for 72 h. Cell extracts were IP with MDM2 or immunodepleted (ID) with MDM2 antibody followed by immunoblotting with the p53 antibody. *C*, immunofluorescence imaging analysis of the subcellular localization of FHIT and MDM2 proteins in A549 cells in which the endogenous expression of p53 was induced by cisplatin followed by transduction with Ad-*FHIT*. Immunofluorescence staining was performed 24 h after transduction. Expression of the FHIT proteins is shown in *green* (FITC) (*a*), MDM2 expression is shown in *red* (rhodamine) (*b*), and nuclei are shown in *blue* 4′,6-diamidino-2-phenylindole (DAPI) (*c*); an overlapped image is shown in *d*. The FHIT protein was mainly detected in cytosol, whereas the MDM2 protein was predominantly located in nuclei. The untransduced (N) and the Ad-*FHIT*-transduced (F) cells are indicated with *arrows*.

a significant synergistic inhibition in the growth of NSCLC cells both *in vitro* and *in vivo*.

There is increasing evidence that the inactivation of multiple tumor suppressor genes has a synergistic effect on tumor development and proliferation (22, 27). For example, >50% of NSCLCs have been found to carry *p53* mutations (11) and 50–70% of NSCLCs also have deficient *FHIT* gene expression (28, 29). In addition, several studies have demonstrated that an allelic imbalance within the *FHIT* locus frequently coexists with *p53* abnormalities and that this may be an early event in NSCLC pathogenesis (30, 31). From a clinical perspective, NSCLCs are highly resistant to conventional treatments such as surgery, radiotherapy, and chemotherapy (32). On the basis of these observations and known facts, combination treatment with synergistic tumor-suppressing gene therapy (in our case, adenoviral vector-mediated *FHIT* and *p53* gene cotransfer) may constitute a rational and effective strategy for the treatment of a wide range of both lung and other cancers.

The stability of p53 is the key to the maintenance of multiple cellular functions such as cell cycle arrest and apoptosis. The *p53* tumor suppressor gene is activated in response to diverse cellular stresses such as those inflicted by DNA-damaging agents and to oncogenic signals through mechanisms that result in the stabilization and accumulation of wild-type p53 protein (20, 33). Overexpression of FHIT protein up-regulated both the endogenous and exogenous wild-type p53 expression in NSCLC cells transduced by the Ad-*FHIT* vector alone or cotransduced by Ad-*FHIT* and Ad-*p53*. However, the latter results in synergistically enhanced tumor suppression and apoptotic activities, which may be a direct reflection of the FHIT-mediated stabilization of p53. This implicates an important molecular pathway in the regulation of FHIT-mediated tumor-suppressing activity. Although the sensitivity of tumor cells to the adenoviral vector-mediated *FHIT* transfer-induced growth inhibition was not significantly correlated with the *p53* gene status in the cells tested (4, 6), the activation of endogenous p53 in cells possessing wild-type *p53* by a chemotherapeutic agent such as cisplatin or the induction of the exogenous expression of *p53* in *p53*-null or mutant cells by a gene therapy agent such as Ad-*p53* could be used to enhance the therapeutic efficacy of Ad-*FHIT* in a wide range of tumor cells. For example, as shown in this study, in the H460 cells with wild-type *p53* pretreated with cisplatin and then transduced with Ad-*FHIT*, the expression of endogenous p53 was induced, the FHIT-mediated stabilization of the p53 protein was massively enhanced, and caspase-9 was activated (Fig. 1*D*). Of further relevance, the induction of apoptosis mediated by Ad-*p53* and Ad-*FHIT* also follows a different time course. That is, a peak apoptotic induction is seen for Ad-*p53* at ~48 h and for Ad-*FHIT* at ~96 h after transduction (33, 34). They also induce apoptosis via different pathways (35). These differences in therapeutic kinetics and molecular function may thus also contribute to the observed synergistic effect of combination treatment with Ad-*FHIT* and Ad-*p53* on both growth inhibition and apoptosis.

Structural and functional analysis of the MDM2 protein has revealed that MDM2 interacts directly with p53 in the NH_2-terminal domains (20, 36). As a result of this interaction, MDM2 directly blocks the transcription factor and a tumor suppressor activity of p53 (37) and targets p53 for degradation by proteolysis (33, 38). It has thus become clear that one way to stabilize and activate p53 in cells is by interrupting the interaction of MDM2 and p53 (39). Ways to do this are suggested by the fact that the activity of MDM2 is also regulated by covalent modifications and by noncovalent regulators, both of which can modulate the ability of MDM2 to bind p53 (19). In particular, two tumor suppressor proteins, human $p16^{Ink4A}$ and murine $p19^{Arf}$ (human $p14^{Arf}$), have been shown to bind to MDM2 and inhibit the MDM2-mediated degradation of p53 (40, 41). We observed a significant reduction of MDM2 proteins in cells cotransduced by Ad-*FHIT* and Ad-*p53* compared with those transduced by Ad-*p53* alone. We also noticed a significant reduction of MDM2-p53 complexes and detected the direct MDM2-FHIT interaction in those cells. These results suggest that the interaction of FHIT with MDM2 may

interfere the association of MDM2 with p53 and, subsequently, interrupt MDM2-medaited p53 degradation. For some reason, however, the effect was evident only in the Ad-*p53* and Ad-*FHIT*-cotransduced cells. Thus, the synergy in FHIT and p53-mediated suppression of tumor growth and induction of apoptosis may be related to the FHIT-stabilized high level of p53 in these cells. FHIT may induce apoptosis by another mechanism in cells with endogenous wild-type p53.

Our data suggest that the FHIT-mediated reduction in MDM2 expression is neither controlled by the down-regulation of *MDM2* mRNA transcription nor by the activation of the proteasome-dependent MDM2 degradation pathway. It also appears that the $p14^{Arf}$ protein is not involved in the FHIT-mediated regulation of MDM2 expression because both H460 and A549 cell lines express no $p14^{Arf}$ protein as a result of a homozygous gene deletion. However, the phosphorylation of MDM2 and the splice isoform expression of MDM2 may regulate MDM2 protein function such that it serves as an E3 enzyme that degrades the p53 protein (42, 43). We examined these possibilities using Western blot analysis, which showed that a different migrating form of the phosphorylated MDM2 protein occurs in the presence of anti-phospho (Ser^{166})-MDM2 antibody in a vector-dose-dependent manner. We also detected different possible splicing isoforms of MDM2 proteins under nonreduced conditions in Ad-*FHIT*-treated cells (data not shown). Although more detailed studies are needed to clarify and confirm these findings, we propose that the overexpression of FHIT probably inactivates the MDM2 protein by inducing a change in the phosphorylation status of the MDM2 protein and promoting cleavage of the protein into a nonfunctional species.

Taken together, our results indicate that the coexpression of the *FHIT* and *p53* tumor suppressor genes promotes a synergistic inhibition of tumor cell growth *in vitro* and *in vivo*. We also identified a novel molecular mechanism for this FHIT-mediated tumor suppression and conclude that FHIT is important to the regulation of p53 because of its ability to interact with other cellular p53 regulators such as MDM2. Our study also points the way for development of novel strategies for cancer gene therapy that involve the combined delivery of two or more tumor suppressor genes that can synergistically induce apoptosis in cancer cells with a defined genotype.

ACKNOWLEDGMENTS

We thank Dr. Guillermina Lozano at The University of Texas M. D. Anderson Cancer Center for her helpful comments on the manuscript.

REFERENCES

1. Lerman MI, Minna JD. The 630-kb lung cancer homozygous deletion region on human chromosome 3p21.3: identification and evaluation of the resident candidate tumor suppressor genes. The International Lung Cancer Chromosome 3p21.3 Tumor Suppressor Gene Consortium. Cancer Res 2000;60:6116–33.
2. Croce CM, Sozzi G, Huebner K. Role of FHIT in human cancer. J Clin Oncol 1999;17:1618–24.
3. Barnes LD, Garrison PN, Siprashvili Z, et al. Fhit, a putative tumor suppressor in humans, is a dinucleoside 5′,5‴-P-1,P-3-triphosphate hydrolase. Biochemistry 1996; 35:11529–35.
4. Ji L, Fang B, Yen N, Fong K, Minna JD, Roth JA. Induction of apoptosis and inhibition of tumorigenicity and tumor growth by adenovirus vector-mediated fragile histidine triad (FHIT) gene overexpression. Cancer Res 1999;59:3333–9.
5. Sard L, Accornero P, Tornielli S, et al. The tumor suppressor gene FHIT is involved in the regulation of apoptosis and in cell cycle control. Proc Natl Acad Sci USA 1999;96:8489–92.
6. Ishii H, Dumon KR, Vecchione A, et al. Effect of adenoviral transduction of the fragile histidine triad gene into esophageal cancer cells. Cancer Res 2001;61:1578–84.
7. Fong LYY, Fidanza V, Zanesi N, et al. Muir-Torre-like syndrome in Fhit-deficient mice. Proc Natl Acad Sci USA 2000;97:4742–7.
8. Dumon KR, Ishii H, Fong LYY et al. FHIT gene therapy prevents tumor development in Fhit-deficient mice. Proc Natl Acad Sci USA 2001;98:3346–51.
9. Levine AJ. p53, the cellular gatekeeper for growth and division. Cell 1997;88:323–31.
10. Hollstein M, Sidransky D, Vogelstein B, Harris CC. p53 mutations in human cancers. Science (Wash DC) 1991; 1991;253:49–53.
11. Brambilla E, Gazzeri S, Lantuejoul S, et al. p53 mutant immunophenotype and deregulation of p53 transcription pathway (Bcl2, Bax, and Waf1) in precursor bronchial lesions of lung cancer. Clin Cancer Res 1998;4:1609–18.
12. Harris CC. Structure and function of the p53 tumor suppressor gene: clues for rational cancer therapeutical strategies. J Natl Cancer Inst (Bethesda) 1999;88:1442–55.
13. Roth JA, Nguyen D, Lawrence DD. et al. Retrovirus-mediated wild-type p53 gene transfer to tumors of patients with lung cancer. Nat Med 1996;2:985–91.
14. Roth JA, Grammer SF, Swisher SG, Nemunaitis J, Merritt J, Meyn RE Jr. Gene replacement strategies for treating non-small cell lung cancer. Semin Radiat Oncol 2000;10:333–42.
15. Swisher SG, Roth JA, Komaki R, et al. Induction of p53 regulated genes and tumor regression in lung cancer following intratumoral delivery of adenoviral p53 (RPR/INGN 201) and radiation therapy. Clin Cancer Res 2002;9:93–101.
16. Lowe SW, Bodis S, McClatchey A. et al. p53 status and the efficacy of cancer therapy *in vivo*. Science (Wash DC) 1994;266:807–10.
17. Ashcroft M, Vousden KH. Regulation of p53 stability. Oncogene 1999;18:7637–43.
18. Caspari T. How to activate p53. Curr Biol 2000;10:R315–7.
19. Juven-Gershon T Oren M. Mdm2: the ups and downs. Mol Med 1999;5:71–83.
20. Freedman DA, Levine AJ. Regulation of the p53 protein by the MDM2 oncoprotein: thirty-eighth G. H. A. Clowes Memorial Award Lecture. Cancer Res 1999;59:1–7.
21. Yu ZK, Geyer RK, Maki CG. MDM2-dependent ubiquitination of nuclear and cytoplasmic P53. Oncogene 2000;19:5892–7.
22. Garinis GA, Gorgoulis VG, Mariatos G, et al. Association of allelic loss at the FHIT locus and p53 alterations with tumour kinetics and chromosomal instability in non-small cell lung carcinomas (NSCLCs). J Pathol 2001;193:55–65.
23. Steel GG, Peckham MJ. Exploitable mechanisms in combined radiotherapy-chemotherapy: the concept of additivity. Int J Radiat Oncol Biol Phys 1997;5:85–91.
24. Soriano P, Montgomery C, Geske R, Bradley A. Targeted disruption of the c-src proto-oncogene leads to osteopetrosis in mice. Cell 1991;64:693–702.
25. Nishizaki M, Meyn RE, Levy LB, et al. Synergistic inhibition of human lung cancer cell growth by adenovirus-mediated wild-type p53 gene transfer in combination with docetaxel and radiation therapeutics *in vitro* and *in vivo*. Clin Cancer Res 2001;7: 2887–97.
26. Ashcroft M, Kubbutat MH, Vousden KH. Regulation of p53 function and stability by phosphorylation. Mol Cell Biol 1999;19:1751–8.
27. Serrano M, Lin AW, McCurrach ME, Beach D, Lowe SW. Oncogenic ras provokes premature cell senescence associated with accumulation of p53 and p16INK4a. Cell 1997;88:593–602.
28. Sozzi G, Pierotti MA. When smoke gets in your genes. Nat Med 1998;4:1119–20.
29. Sozzi G, Huebner K, Croce CM. FHIT in human cancer. Adv Cancer Res 1998;74: 141–66.
30. Marchetti A, Pellegrini S, Bertacca G, et al. Fhit and p53 gene abnormalities in bronchioloalveolar carcinomas: correlations with clinicopathological data and K-ras mutations. J Pathol 1998;184:240–6.
31. Marchetti A, Pellegrini S, Sozzi G, et al. Genetic analysis of lung tumours of non-smoking subjects: p53 gene mutations are constantly associated with loss of heterozygosity at FHIT locus. Br J Cancer 1998;78:73–8.
32. Roth JA. Gene replacement strategies for lung cancer. Curr Opin Oncol 1998;10: 127–32.
33. Haupt Y, Maya R, Kazaz A, Oren M. Mdm2 promotes the rapid degradation of p53. Nature (Lond.) 1997;387:296–9.
34. Pearson AS, Spitz FR, Swisher SG. et al. Up-regulation of the proapoptotic mediators bax and bak after adenovirus-mediated *p53* gene transfer in lung cancer cells. Clin Cancer Res 2000;6:887–90.
35. Roz L, Gramegna M, Ishii H, Croce CM, Sozzi G. Restoration of fragile histidine triad (FHIT) expression induces apoptosis and suppresses tumorigenicity in lung and cervical cancer cell lines. Proc Natl Acad Sci USA 2002;99:3615–20.
36. Freedman DA, Epstein CB, Roth JC, Levine AJ. A genetic approach to mapping the p53 binding site in the MDM2 protein. Mol Med 1997;3:248–59.
37. Chen L, Agrawal S, Zhou W, Zhang R, Chen J. Synergistic activation of p53 by inhibition of MDM2 expression and DNA damage. Proc Natl Acad Sci USA 1998; 95:195–200.
38. Kubbutat MH, Jones SN, Vousden KH. Regulation of p53 stability by Mdm2. Nature (Lond.) 1997;387:299–303.
39. Prives C. Signaling to p53: breaking the MDM2–p53 circuit. Cell 1998;95:5–8.
40. Weber JD, Taylor LJ, Roussel MF, Sherr CJ, Bar-Sagi D. Nucleolar Arf sequesters Mdm2 and activates p53. Nat Cell Biol 1999;1:20–6.
41. Weber JD, Kuo ML, Bothner B. et al. Cooperative signals governing ARF-mdm2 interaction and nucleolar localization of the complex. Mol Cell Biol 2000;20:2517–28.
42. Evans SC, Viswanathan M, Grier JD, Narayana M, El Naggar AK, Lozano G. An alternatively spliced HDM2 product increases p53 activity by inhibiting HDM2. Oncogene 2001;20:4041–9.
43. Zhou BP, Liao Y, Xia W, Zou Y, Spohn B, Hung MC. HER-2/neu induces p53 ubiquitination via Akt-mediated MDM2 phosphorylation. Nat Cell Biol 2001;3:973–82.